Supplementary Information Figures

Contents

Figure S1: Food consumption of 5d and 30d survival cohorts

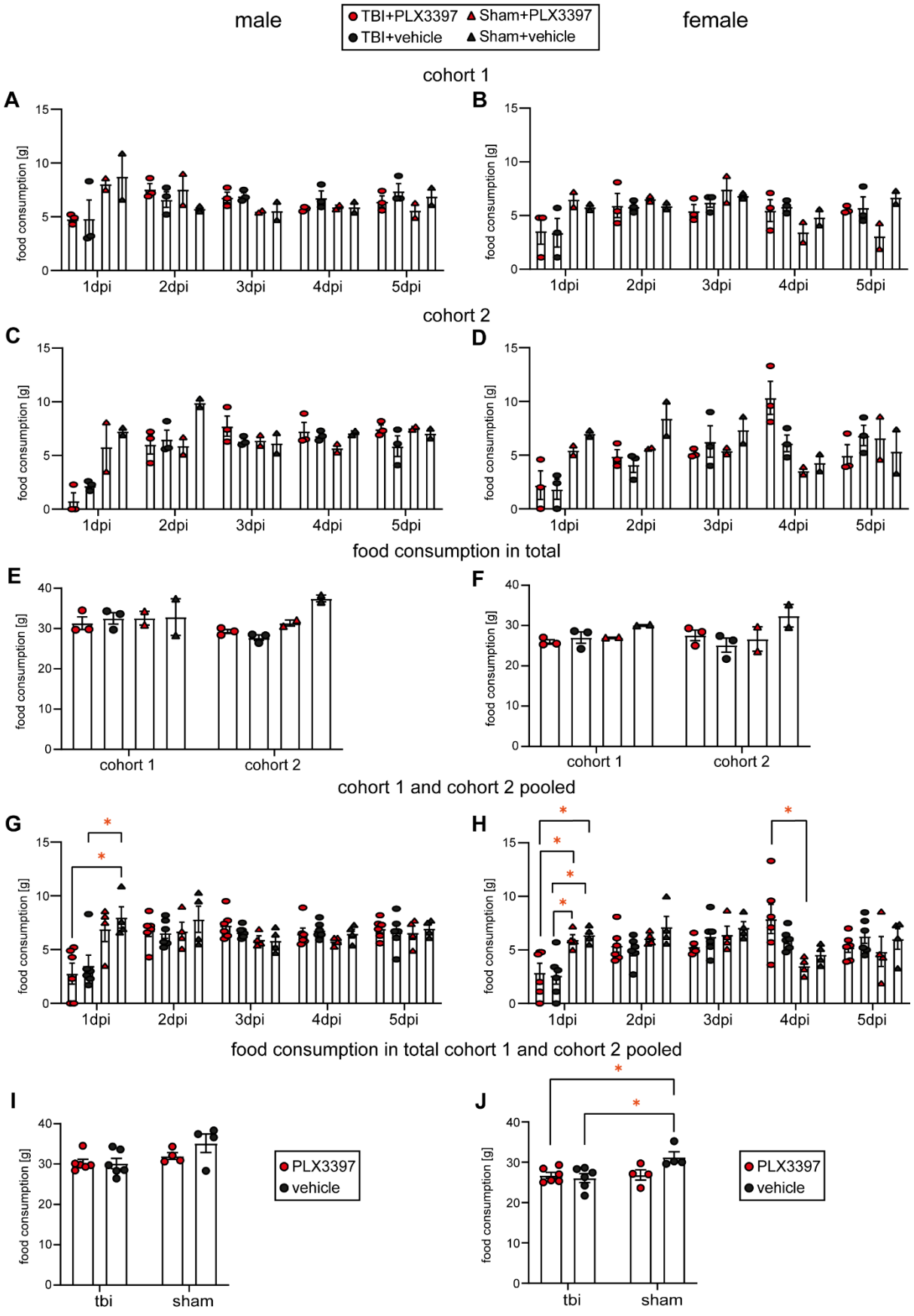

Supplemental Fig. S1: (A, B) Food consumption in male and female mice from 5d survival cohort. (C, D) Food consumption in male and female mice from 30d survival cohort. (E, F) Total food consumption over 5d PLX3397/vehicle treatment in cohort 1 (5d survival) and cohort 2 (30d survival) in male and female mice. (G, H) Food consumption pooled from cohort 1 and cohort 2. (I, J) Total food consumption pooled from cohort 1 and cohort 2. Values from cages (two animals per cage) and mean ± SEM are shown, each scatter is a cage. Significant differences are highlighted, two-way ANOVA followed by Holm Šídák`s multiple comparisons test. *p<0.05. Full statistics are reported in Suppl. Table S2-3.

Figure S2: Body weight of 5d (cohort 1) and 30d survival (cohort 2)

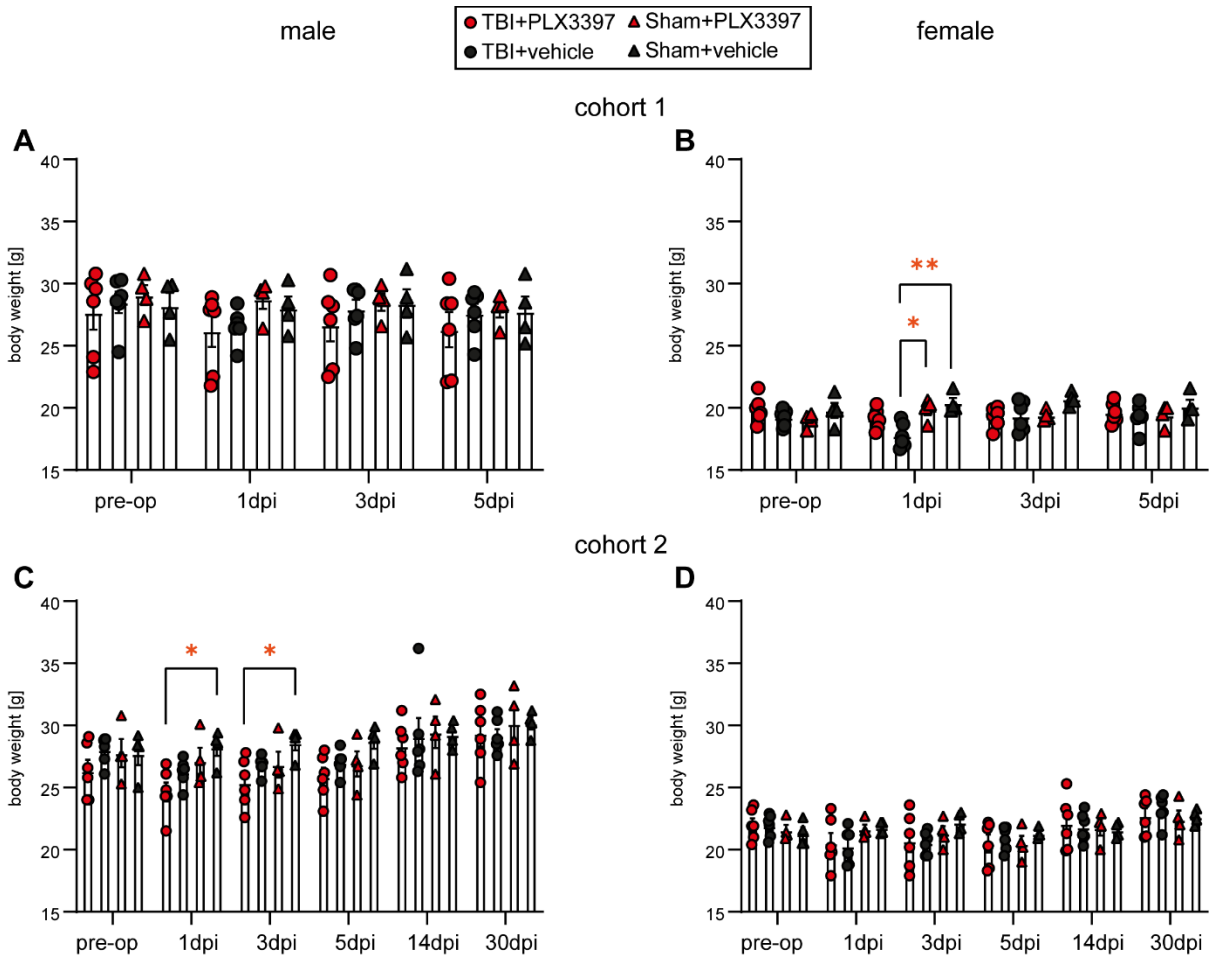

Supplemental Fig. S2: (A, B) Body weight in male and female mice from cohort 1 (5d survival) and cohort 2 (30d survival). Values from individual animals and mean ± SEM are shown, each scatter is a mouse. Significant differences are highlighted, two-way ANOVA followed by Holm Šídák`s multiple comparisons test. *p<0.05, **p<0.01. Full statistics are reported in Suppl. Table S3-3.

Figure S3: Schemes showing brain sections at different Bregma levels collected by serial cryo-sectioning.

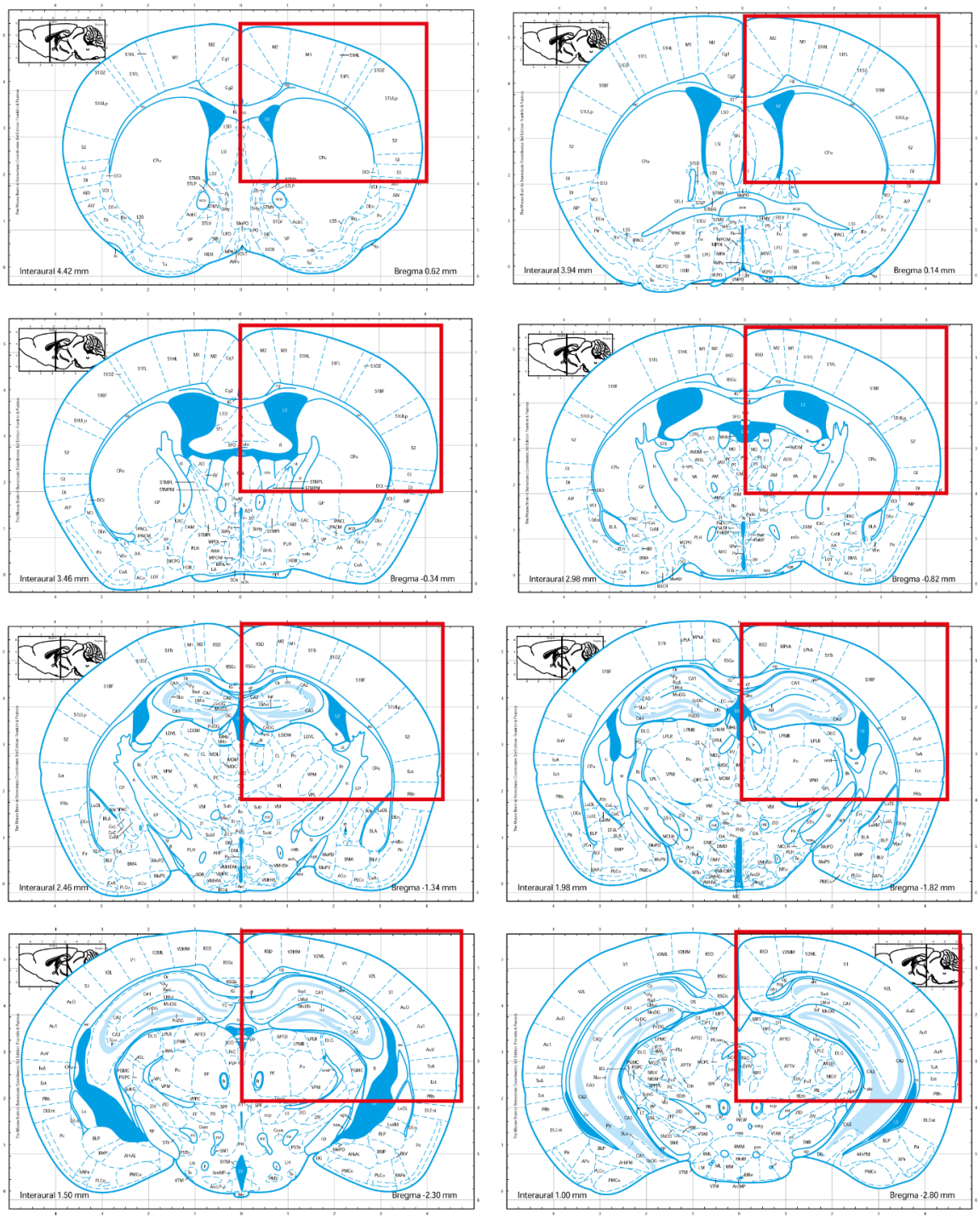

Fig. S3: Schemes showing brain sections at different Bregma levels collected by serial cryosectioning from +0.64 mm to -2.86 mm. Slight deviations from the depicted Bregma levels are due to image availability. Red rectangles indicate regions of interests that were processed for qPCR, Western Blot, or RNA-sequencing from TBI and sham animals (lesions not shown). Images were taken from the Mouse Brain in Stereotaxic Coordinates 3rd Edition Franklin & Paxinos.

Figure S4: Immunohistochemistry of M/M at 5 dpi

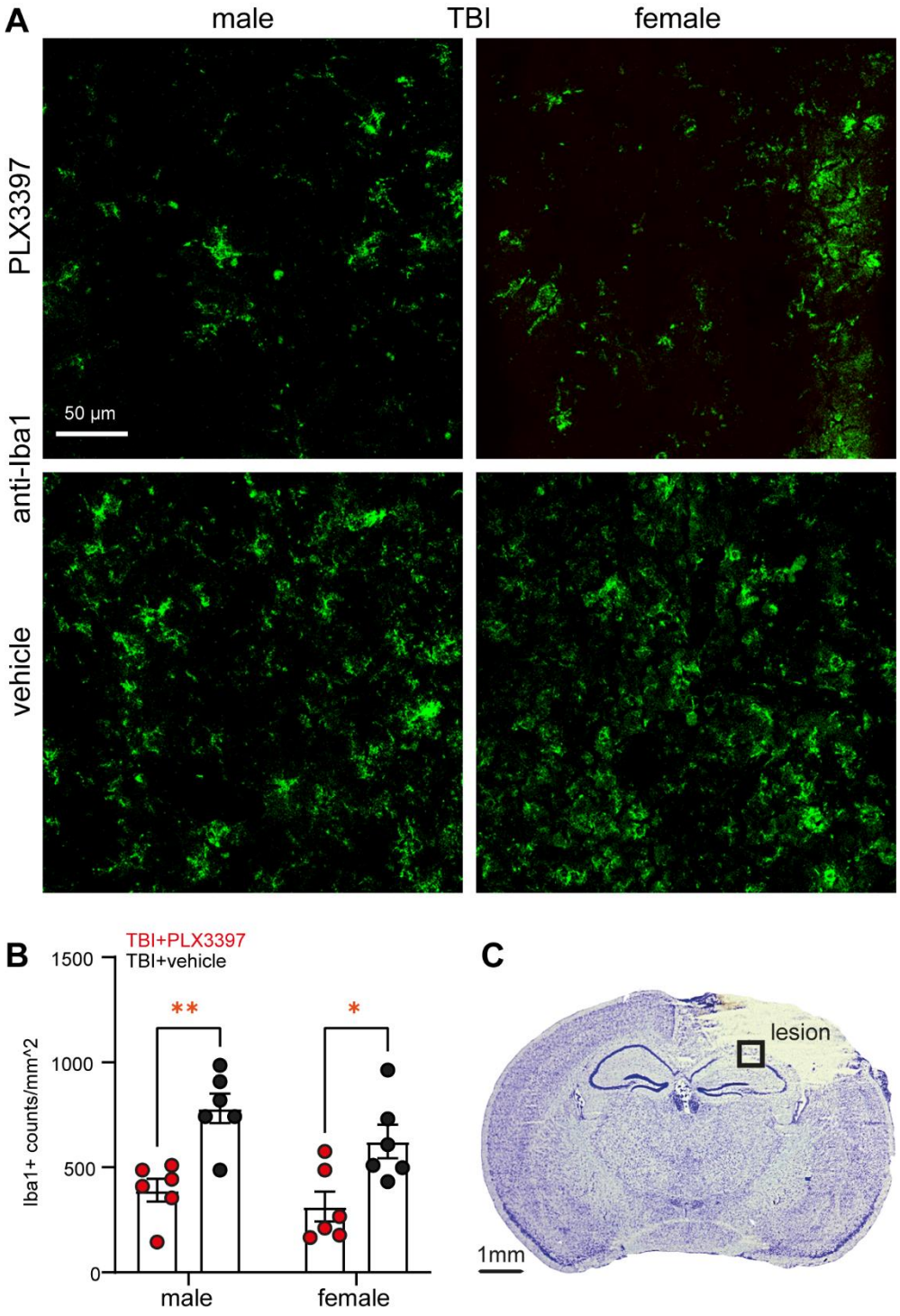

Fig. S4: (A) Anti-Iba1 immunostaining showing that PLX3397 treatment attenuated M/M accumulation at 5 dpi. (B) Histogram showing that Iba1$^+$ M/M were reduced approximately 50% by PLX3397 treatment in both male and females at 5 dpi (TBI: n=6, per group, equal sex ratios). Significant differences are highlighted, Student's unpaired two-tailed t test. Values from individual animals and mean ± SEM are shown. *p<0.05, **p<0.01. Scale: 50 µm (A), 1mm (C). Full statistics are reported in Suppl. Table S6.

1 **Figure S5: Immunohistochemistry of M/M and astrocytes at 30 dpi**

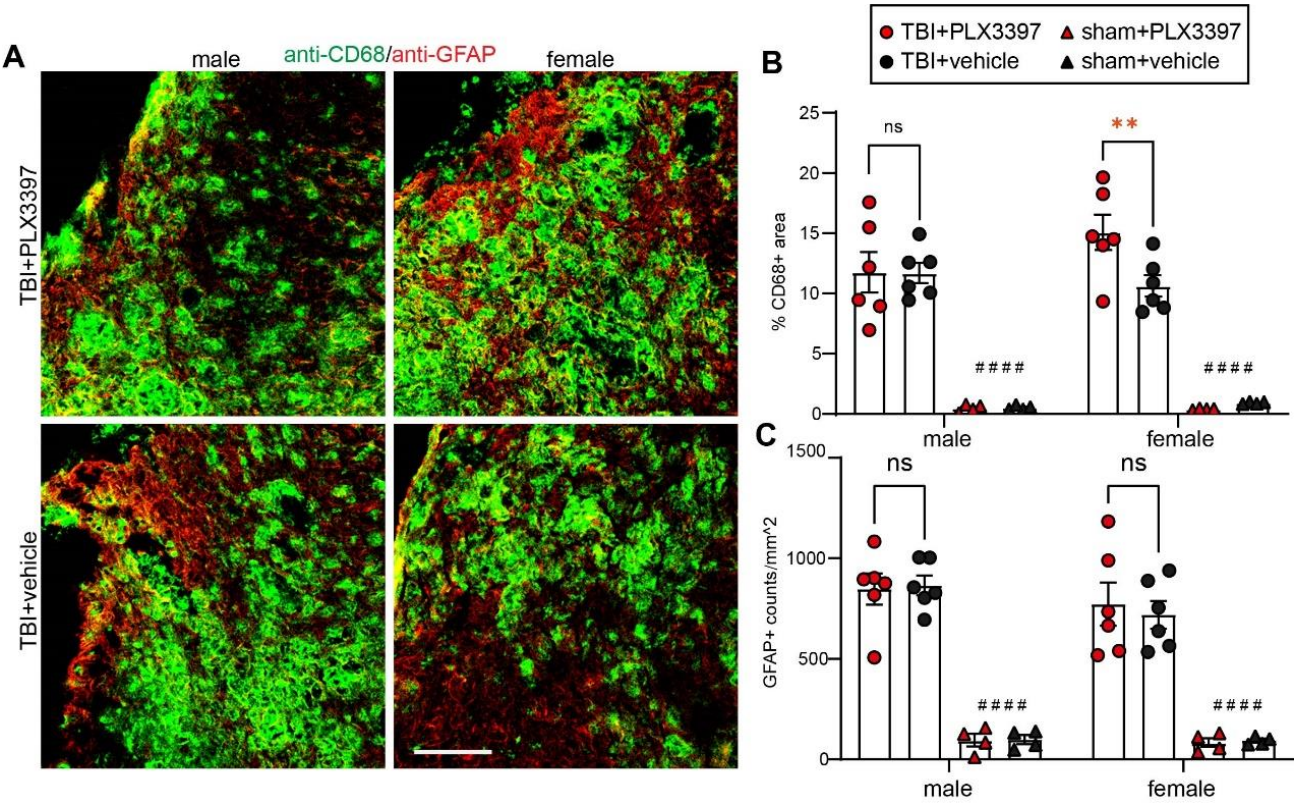

Fig. S5: (A) Anti-CD68/anti-GFAP double-immunostaining showing repopulation of M/M and sustained astrogliosis at 30 dpi. (B, C) Histograms show the percentage area of $CD68^+$ microglia/macrophages. The area of $CD68^+$ microglia/macrophages was increased in TBI PLX3397 females vs. vehicle females (TBI: n=6, sham: n=4, per group, equal sex ratios, two-way ANOVA followed by Holm Šídák`s multiple comparisons test). Values from individual animals and mean ± SEM are shown. Asterisks indicate PLX3397 vs. vehicle, **p<0.01. Crosses indicate TBI vs. sham, ####p<0.0001, ns=not significant. Scale: 100 µm (A). Full statistics are reported in Suppl. Table S7.

2

Figure S6: Heatmap of leading edge differentially expressed genes in TBI mice treated with PLX3397 vs. vehicle

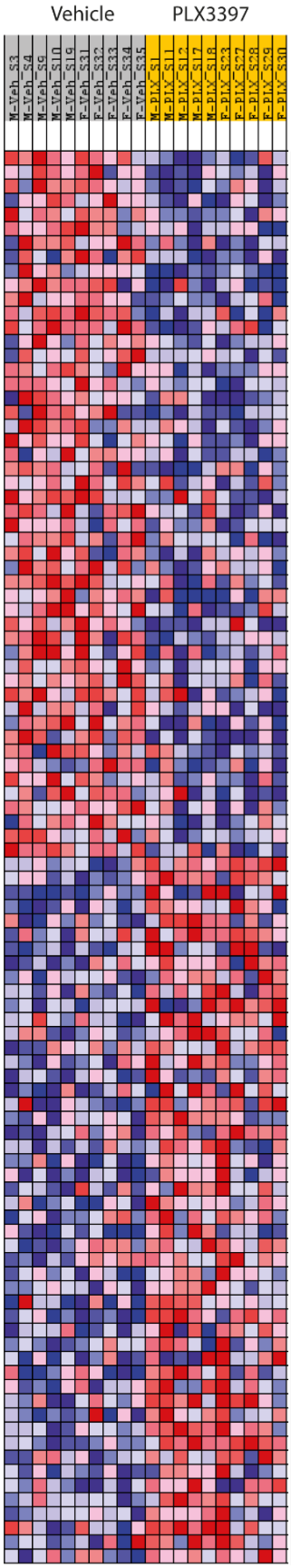

GSEA Leading Edge genes

NAME	TITLE	SCORE
CUZD1	CUB and zona pellucida like domains 1	1.0406524
AWAT2	acyl-CoA wax alcohol acyltransferase 2	0.7762267
BUB1	BUB1 mitotic checkpoint serine/threonine kinase	0.76527816
FANCD2OS	FANCD2 opposite strand	0.70289135
FAM83C	family with sequence similarity 83 member C	0.68971896
FOXD2	forkhead box D2	0.68935114
CIBAR2	CBY1 interacting BAR domain containing 2	0.6783367
C11orf16	chromosome 11 open reading frame 16	0.6722499
ACCSL	1-aminocyclopropane-1-carboxylate synthase homolog (inactive) like	0.6547417
LIPH	lipase H	0.6507007
C1RL	complement C1r subcomponent like	0.63184565
DOK2	docking protein 2	0.6306571
SHISAL2B	shisa like 2B	0.6275896
ATP6V1C2	ATPase H+ transporting V1 subunit C2	0.6264042
CFAP73	cilia and flagella associated protein 73	0.6166859
NEK5	NIMA related kinase 5	0.6071918
EDA2R	ectodysplasin A2 receptor	0.606794
KCNK7	potassium two pore domain channel subfamily K member 7	0.597321
GPR160	G protein-coupled receptor 160	0.58900946
KRT15	keratin 15	0.5836542
KCNJ5	potassium inwardly rectifying channel subfamily J member 5	0.57574457
MIS18BP1	MIS18 binding protein 1	0.5718744
APOC3	apolipoprotein C3	0.56824815
CES1	carboxylesterase 1	0.56725043
ANKRD2	ankyrin repeat domain 2	0.56548345
LRP2BP	LRP2 binding protein	0.5647875
CDC25C	cell division cycle 25C	0.56081975
CLTRN	collectrin, amino acid transport regulator	0.5606576
C5	complement C5	0.5540898
SMIM5	small integral membrane protein 5	0.5482738
CABCOCO1	ciliary associated calcium binding coiled-coil 1	0.5476003
TESMIN	testis expressed metallothionein like protein	0.5472343
CDC20	cell division cycle 20	0.54701966
KNTC1	kinetochore associated 1	0.5455193
SNCG	synuclein gamma	0.54506016
RSPH14	radial spoke head 14 homolog	0.5442772
LRRC71	leucine rich repeat containing 71	0.54169005
CFAP157	cilia and flagella associated protein 157	0.537231
AFMID	arylformamidase	0.5354919
APOA2	apolipoprotein A2	0.53428584
CFAP126	cilia and flagella associated protein 126	0.52842134
BBOX1	gamma-butyrobetaine hydroxylase 1	0.5274359
MBOAT4	membrane bound O-acyltransferase domain containing 4	0.5268612
LYG2	lysozyme g2	0.5261924
PROKR2	prokineticin receptor 2	0.52575994
LEFTY2	left-right determination factor 2	0.52539474
FAM166B	family with sequence similarity 166 member B	0.5240629
FAM47E-STBD1	FAM47E-STBD1 readthrough	0.52292717
CHODL	chondrolectin	0.51988906
ZNF438	zinc finger protein 438	0.5186722
DCAF12L2	DDB1 and CUL4 associated factor 12 like 2	-0.7858888
ZBTB32	zinc finger and BTB domain containing 32	-0.7754126
ZP3	zona pellucida glycoprotein 3	-0.6681483
ZG16B	zymogen granule protein 16B	-0.6582309
C20orf202	chromosome 20 open reading frame 202	-0.6389216
PLA2G2F	phospholipase A2 group IIF	-0.62882733
FBP2	fructose-bisphosphatase 2	-0.61040837
MYBPC1	myosin binding protein C1	-0.60837996
FSTL3	follistatin like 3	-0.6018477
LCT	lactase	-0.597616
GEMIN4	gem nuclear organelle associated protein 4	-0.58609533
LIF	LIF interleukin 6 family cytokine	-0.57896525
UPK1B	uroplakin 1B	-0.5783265
SLC23A4P	solute carrier family 23 member 4, pseudogene	-0.5734411
CACNG1	calcium voltage-gated channel auxiliary subunit gamma 1	-0.56803983
APOF	apolipoprotein F	-0.56694543
ADGRD1	adhesion G protein-coupled receptor D1	-0.56277865
KASH5	KASH domain containing 5	-0.56107396
PLIN4	perilipin 4	-0.553751
LRG1	leucine rich alpha-2-glycoprotein 1	-0.5508636
IFI27L2	interferon alpha inducible protein 27 like 2	-0.5253784
SLFN13	schlafen family member 13	-0.5248041
IRF7	interferon regulatory factor 7	-0.5242461
DSP	desmoplakin	-0.51935667
UNC45B	unc-45 myosin chaperone B	-0.51637775
NXF2B	nuclear RNA export factor 2B	-0.5138136
HSPA1B	heat shock protein family A (Hsp70) member 1B	-0.50898105
PCDHB2	protocadherin beta 2	-0.50350374
SMIM22	small integral membrane protein 22	-0.5022136
RSAD2	radical S-adenosyl methionine domain containing 2	-0.49085754
CYTL1	cytokine like 1	-0.48846218
LCTL	lactase like	-0.48834452
ABRAXAS1	abraxas 1, BRCA1 A complex subunit	-0.4863127
POU2AF1	POU class 2 homeobox associating factor 1	-0.48620453
GRAP2	GRB2 related adaptor protein 2	-0.48571894
TPSAB1	tryptase alpha/beta 1	-0.48557717
GLP2R	glucagon like peptide 2 receptor	-0.48524523
B3GNT4	UDP-GlcNAc:betaGal beta-1,3-N-acetylglucosaminyltransferase 4	-0.4842957
SHC3	SHC adaptor protein 3	-0.48294863
SH2D4B	SH2 domain containing 4B	-0.4761375
ADCY1	adenylate cyclase 1	-0.47550845
TMEM132D	transmembrane protein 132D	-0.47448778
CD101	CD101 molecule	-0.47388098
OASL2P	2'-5' oligoadenylate synthetase like 2, pseudogene	-0.4707648
NPHS1	NPHS1 adhesion molecule, nephrin	-0.4698216
LGALS3BP	galectin 3 binding protein	-0.4682616
PHF11	PHD finger protein 11	-0.46717808
GPR63	G protein-coupled receptor 63	-0.46640754
MYBPH	myosin binding protein H	-0.4657669
PIWIL2	piwi like RNA-mediated gene silencing 2	-0.4649337

Fig. S6: Heatmap of leading edge differentially expressed genes in TBI mice treated with PLX3397 vs. vehicle. Mice were treated with the CSF1R inhibitor PLX3397 (n = 5 male, 5 female) or vehicle (n = 5 male, 5 female) for five days after TBI. Brain tissue of the ipsilateral upper quadrant was collected at 30 dpi and analysed per RNAseq. Gene set enrichment analysis was done with an input of 16970 valid genes using GSEA 4.1.0 (https://www.gsea-msigdb.org/gsea/index.jsp), and 14980 gene were successfully ranked according to fold regulation and P-value. Leading edge 50 upregulated and 50 downregulated genes are presented in red to blue colour showing high to low relative expression.

Figure S7: Gene enrichment plots of GSEA gene sets in TBI mice treated with PLX3397 vs. vehicle

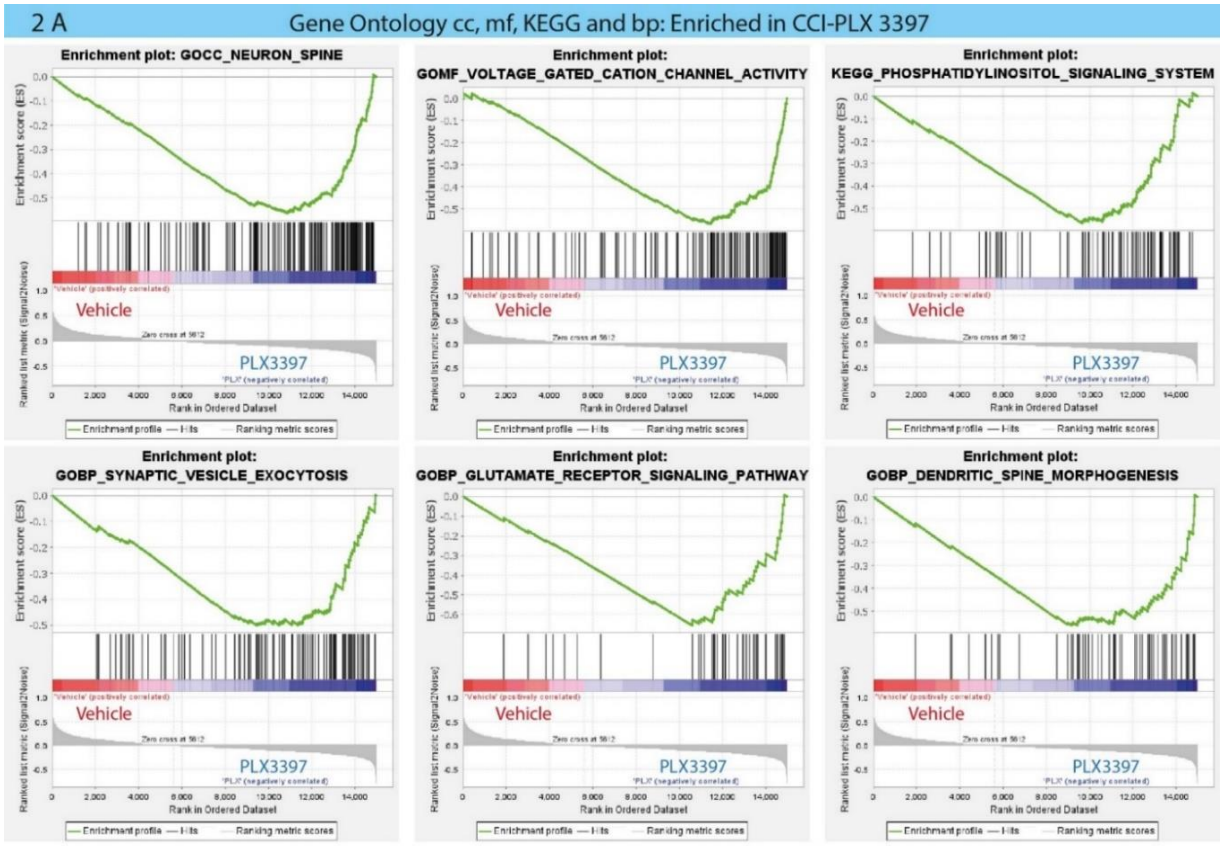

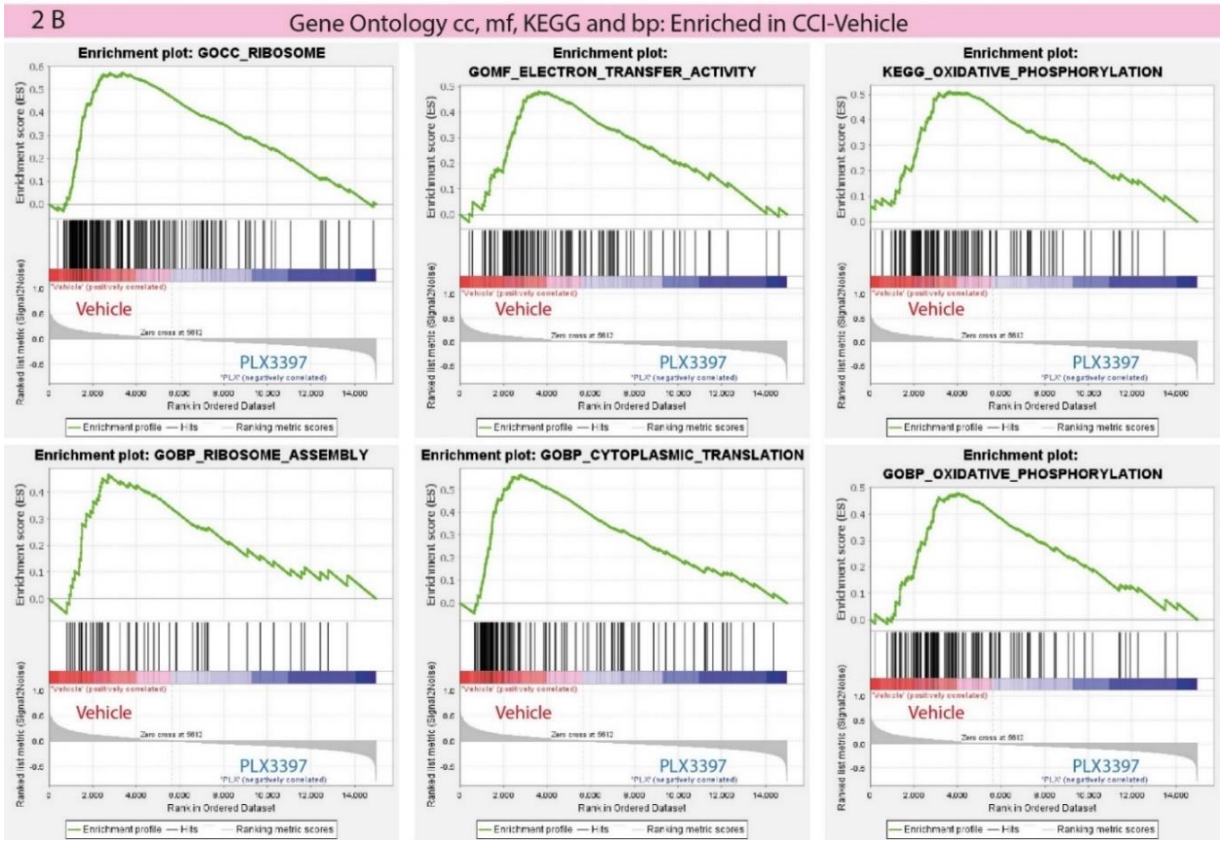

Fig. S7: Gene enrichment plots of GSEA gene sets in TBI mice treated with PLX3397 versus vehicle. Mice were treated as described in Suppl. Fig. S2 (above), and gene set enrichment analysis was run with GSEA 4.1.0 for the gene sets KEGG, GOcc, GOmf and GObp (GO, gene ontology; cc, cellular component; mf, molecular function; bp, biological process). Enrichment plots show the enrichment score of a given gene in the set. The green line represents the running ES as the analysis goes down the ranked list. The value at the peak is the final ES. Genes enriched in vehicle treated mice are depicted as positive ES (red), genes enriched in PLX3397 treated mice are depicted as negative ES in blue.

Figure S8: Exemplary heatmaps of gene sets enriched in TBI mice treated with PLX3397

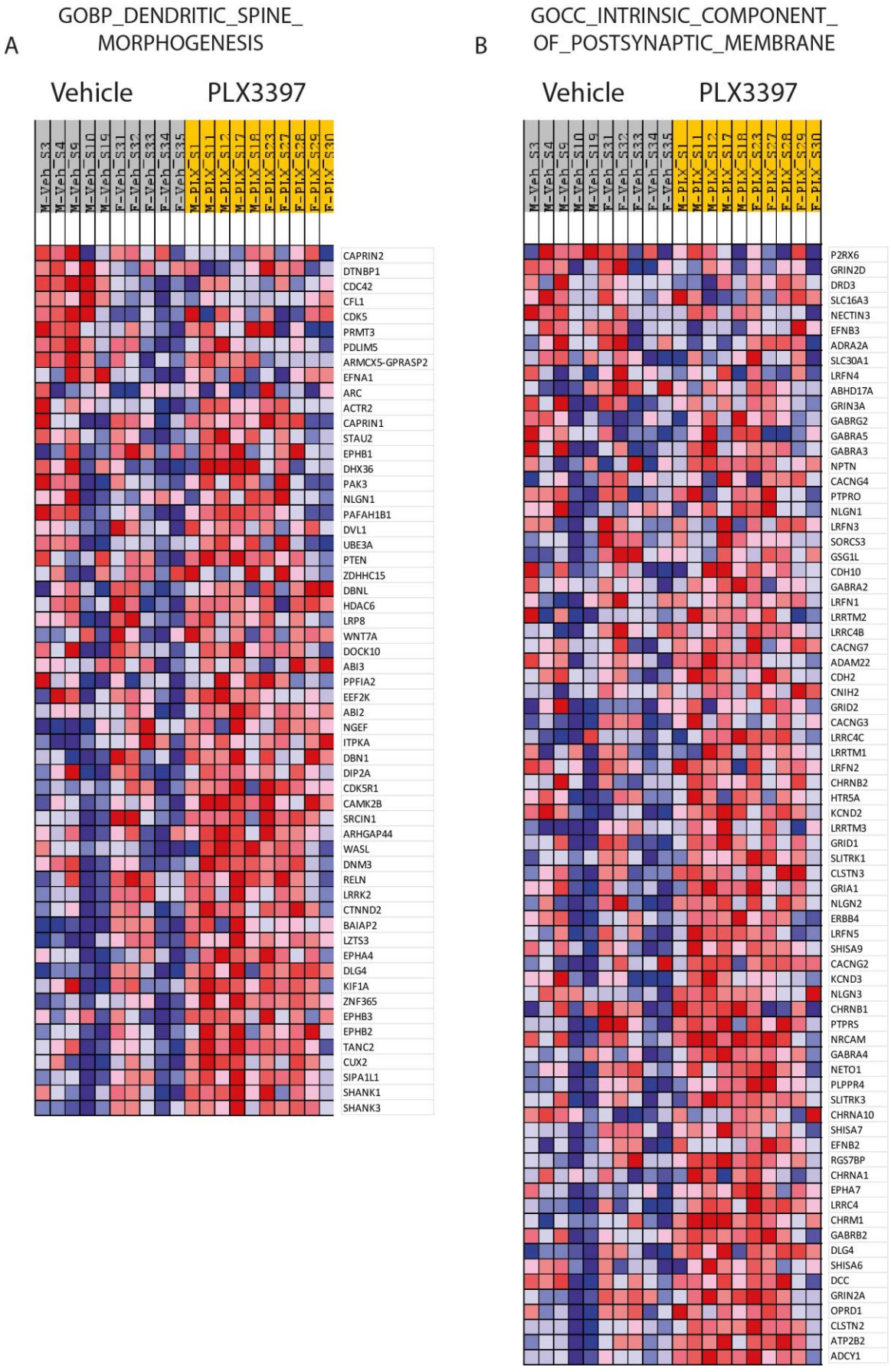

Fig. S8: Exemplary heatmaps of genes enriched in TBI mice treated with PLX3397. Mice were treated as described in Suppl. Fig.2 (above). Gene sets of synapse, postsynaptic membrane, synaptic vesicle exocytosis, axonal membrane, spine development and similar synaptic terms were enriched in PLX3397-treated TBI mice relative to vehicle-treated TBI mice. Two exemplary heat maps are presented. The colour code ranges from high enrichment score (ES) in dark red to low ES in dark blue.

Figure S9: Exemplary heatmaps of genes enriched in TBI mice treated with vehicle

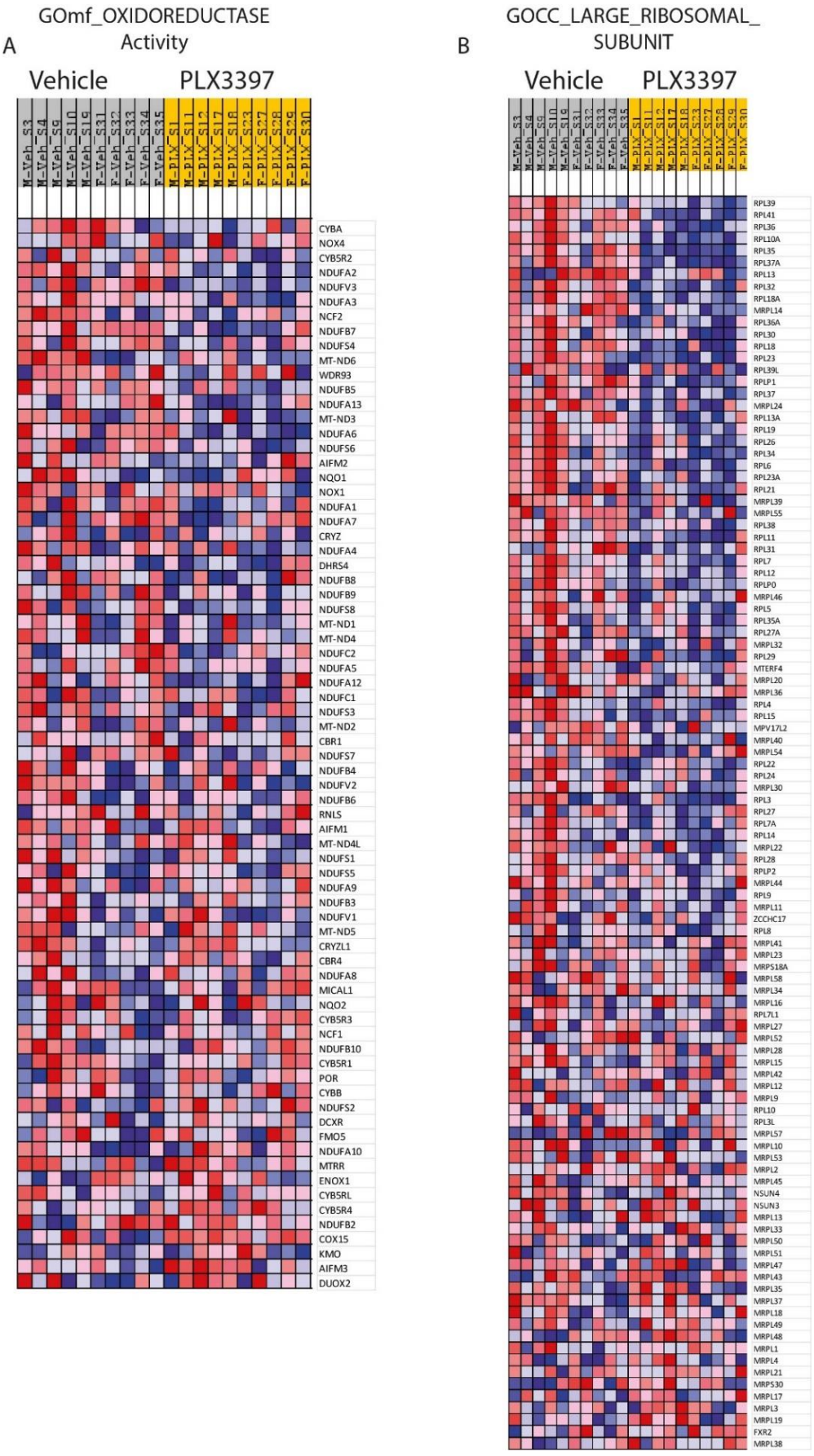

Fig. S9: Exemplary heatmaps of gene sets enriched in TBI mice treated with vehicle. Mice were treated as described in Suppl. Fig. S2 (above). Gene sets of ribosome, ribosomal subunit, cytoplasmic translation were enriched in vehicle treated mice and terms of oxidoreductase activity, oxidative phosphorylation or electron transfer were enriched in vehicle treated mice. Two exemplary heat maps are presented. The colour code ranges from high enrichment score (ES) in dark red to low ES in dark blue.

Figure S10: Scatter plot and heatmap of top regulated genes according to p-value/q-value

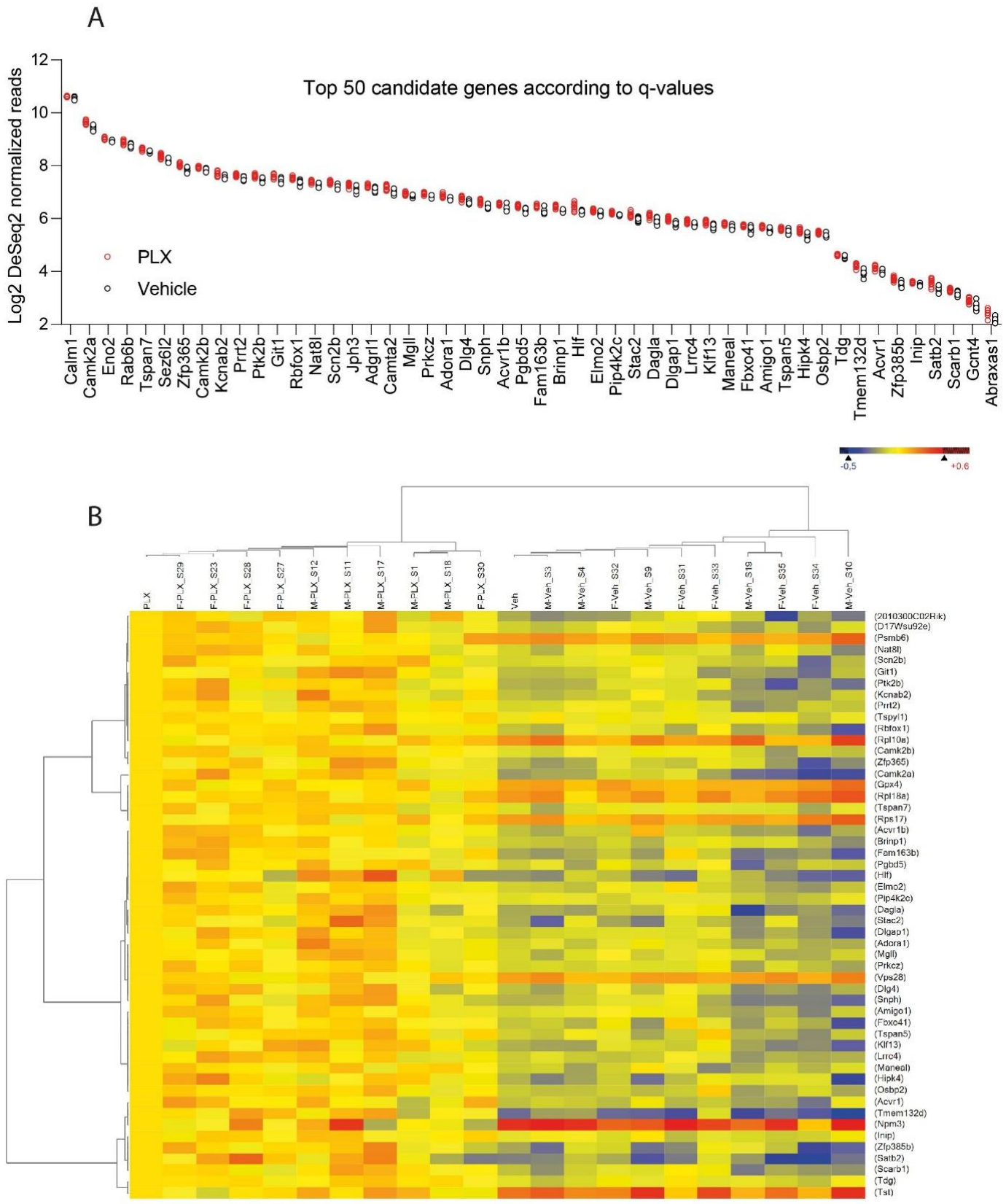

Hierarchical clustering, Euclidean distance metrics, ttest significant genes

Fig.S10: Scatter plot and heatmap of top regulated genes according to p-value/q-value. (A) Scatter plot of top 50 regulated genes according to FDR adjusted p-value (q-value) sorted for abundance. The data are log2 transformed normalized reads. (B) Heatmap showing the relative expression vs. the mean of PLX3397-treated mice (left column) of Student`s t test significant regulated genes in PLX3397-treated TBI mice vs. vehicle-treated TBI mice. Genes and mice were clustered according to Euclidean distance metrics. The colour scale ranges from minus 3.5-fold SD to plus 3.5-fold SD. The upper dendrogram shows two clusters reflecting the treatment groups.

Figure S11: Comparison of sexes of RNAseq data

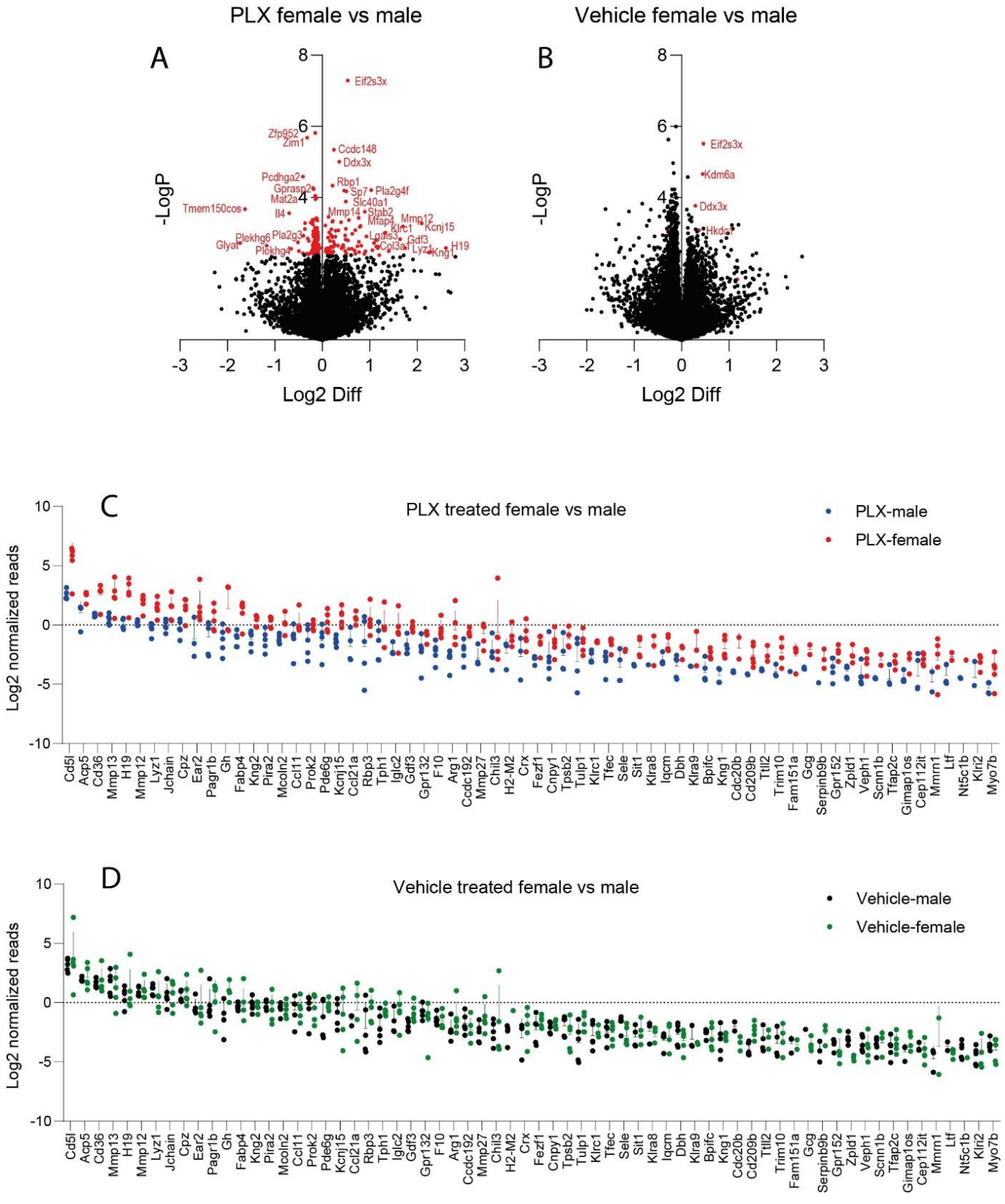

Fig. S11: Comparison of sexes of RNAseq data. Mice were treated with the Csf1R inhibitor PLX3397 (n = 5 male, 5 female) or vehicle (n = 5 male, 5 female) for five days after controlled cortical impact (CCI). Brain

tissue of the ipsilateral upper quadrant was collected 30 days after CCI and subjected to RNAseq analysis. (A): Volcano plots of differential gene expression in PLX-treated female versus PLX-treated male mice The X-axis shows the log2 difference (i.e. fold difference). Genes higher in PLX-treated female mice are positive, genes lower in females are negative. The Y-axis shows the negative logarithm of the P-value. Top 150 candidate according to P-value are highlighted in red. (B): In analogy to A, the Volcano plots shows gene expression in vehicle treated female versus vehicle-treated male mice. The same genes were marked in red as in A, but are mostly hidden because they were not regulated. Few regulated red genes are X-chromosome genes. Y-chromosome genes were excluded. (C): Exemplary scatter plots of candidate genes which were upregulated in PLX3397 treated female mice over PLX-treated male mice. The genes were filtered according to fold difference (Log2 difference ≥1.3 for PLX-female > PLX male) and are sorted left to right according to abundance (normalized reads). (D): Genes as in C comparing vehicle treated female versus vehicle treated male mice.

Figure S12: Exemplary heatmap of genes enriched in PLX3397-treated female vs. male TBI mice

Fig.S12: Exemplary heatmaps of Top 50 genes enriched in PLX3397-treated female vs. male TBI mice. Mice were treated as described in Suppl. Fig.2 (above). The colour code ranges from high enrichment score (ES) in dark red to low ES in dark blue.